JOURNAL OF Materials CHEMISTRY

Nickel oxide as a new inhibitor of vanadium-induced hot corrosion of superalloys—comparison to MgO-based inhibitor

E. Rocca,*[a] L. Aranda,[a] M. Moliere[b] and P. Steinmetz[a]

[a]*Université Henri Poincaré-Nancy I, Laboratoire de Chimie du Solide Minéral, UMR CNRS 7555, B.P. 239-54506 Vandoeuvre-Lès-Nancy, France. E-mail: emmanuel.rocca@lcsm.uhp-nancy.fr*
[b]*GE Energy Products-Europe, 1, avenue Charles Bohn, B.P. 379-90007 Belfort, France*

Received 13th June 2002, Accepted 10th September 2002
First published as an Advance Article on the web 15th October 2002

The combustion of vanadium- and sodium-contaminated fuels in gas turbines provokes an accumulation of ash on metallic surfaces of the hot gas path. This ash material causes fouling and corrosion as a result of the formation of low melting point reactive compounds. This paper presents comparative investigations into the effects of adding nickel oxide and magnesium oxide to inhibit this form of high temperature corrosion. The chemistry in corrosive Na_2SO_4–V_2O_5 ash materials is discussed in terms of acid–base reactions in the presence or absence of SO_3 gas using Lux–Flood acid–base theory. It has been found that the addition of NiO leads to the formation of $Ni_3V_2O_8$, a refractory compound that dramatically reduces the corrosiveness of the ash materials by trapping vanadium. In contrast, the effect of MgO on the ash materials is to stabilise the vanadium by reacting with orthovanadate anions (VO_4^{3-}) to form $NaMg_4(VO_4)_3$, which dramatically lowers the corrosive effect. However, the sulfation of a fraction of the MgO results in compaction of the ash materials on the metallic parts, which means that frequent cleaning of the machine is required. It is concluded that nickel oxide is an efficient alternative to magnesium as an inhibitor of hot vanadium corrosion, even in presence of sodium.

Introduction

In recent years, gas turbines have become the equipment of choice for power generation because of the availability of cheap fuel, the short lead times and the ease of installation and flexibility of gas turbine plants. However, in most cases, the use of heavy or contaminated fuels in such combustion equipment is the life-limiting factor for the metallic parts constituting the hot gas path.

The main impurities in these fuels are vanadium and sulfur, which originate from crude oil, and sodium, which comes from contamination during extraction or transport. Ash particles that result from combustion of these impurities preferentially deposit on the blades and vanes of the thermal equipment, and form an ash material composed of complex mixtures of vanadium pentoxide (V_2O_5) and sodium sulfate (Na_2SO_4) that exhibit low melting points, down to 600 °C.[1–3] The resulting molten salt film forms a dangerous corrosive layer, which acts as an ion electrolyte and leads to rapid attack of superalloys.[4–6]

Despite extensive studies devoted to determining the corrosive effects of molten salts in gas turbines or other combustion equipment, the corrosion mechanisms underlying the damage-causing processes remain very complex and difficult to control.[7–10]

The presence of vanadium in ash material containing sodium sulfate seems to increase the oxidising character of the melt due to the presence of the redox couple V^V/V^{IV} (VO_3^-/VO_3^{2-}),[11,12] and to increase the ionic conductivity as a result of rapid O^{2-} exchange between the different vanadium(v) oxide species, $VO_4^{3-}/VO_3^-/V_2O_5$, which favours oxide transport across the salt film.[13] Thus, the corrosive effect of vanadium pentoxide is linked to an increase in the acidic dissolution of the protective oxides of superalloys, such as Cr_2O_3 or Al_2O_3, which get trapped by O^{2-} anions into orthovanadate compounds:

$$Cr_2O_3(s) + V_2O_5(l) \rightarrow 2CrVO_4(l)$$

$$Al_2O_3(s) + V_2O_5(l) \rightarrow 2AlVO_4(l)$$

In addition, according to some authors, the corrosiveness of these molten salts dramatically increases with the sodium content, because of the greater ionicity and fluidity of the corrosive liquid enriched with sodium.[2]

The usual approach to limiting vanadium-induced hot corrosion is to trap the corrosive elements in the flame or downstream from the flame into a refractory compound with a high melting point by adding an additive to the fuel which acts as a corrosion inhibitor.[14,15] Since the 70′s, magnesium compounds are the most commonly used additives. They form MgO in the flame and react with V_2O_5 to produce the refractory magnesium orthovanadate $Mg_3V_2O_8$ (T_f = 1074 °C[16]), according to the literature.[17–19] The amount of corrosive phases on the metallic parts is thus dramatically reduced, but the amount of ash material in the thermal equipment is greatly increased. Indeed, a high Mg/V ratio (Mg/V = 3 by mass) compared to the stoichiometric ratio (Mg/V = 0.7 for $Mg_3V_2O_8$) is necessary in practice to obtain maximum inhibition efficiency. Consequently, the addition of large amounts of magnesium-based inhibitor means that frequent cleaning of the hot gas path is required to remove the large quantities of ash material that result. Several authors have attributed the high Mg/V ratio which is required to the partial sulfation of MgO to $MgSO_4$ *via* contact with combustion gas containing SO_2/SO_3 gas.[18–20] Moreover, other authors have remarked that the presence of sodium in fuels disturbs the reaction between MgO and V_2O_5, so the required Mg/V ratio should be increased with the Na/V ratio.[19–21] Despite the widespread use of magnesium-based inhibitors in combustion facilities, only a few papers report comprehensive studies of

 DOI: 10.1039/b205746h

Table 1 X-Ray diffraction analysis of different oxide melts with an Na/V ratio of 1.5 after 3 days at 850 °C in air containing 150 ppmw SO_3

Mg/V ratio	0.7	3	10
XRD analysis	$NaMg_4(VO_4)_3$–$Na_6Mg(SO_4)_4$–$Mg(VO_3)_2$	MgO–$Na_6Mg(SO_4)_4$ $NaMg_4(VO_4)_3$	MgO–$NaMg_4(VO_4)_3$ $Na_6Mg(SO_4)_4$
Ni/V ratio	1.74	2.25	3
XRD analysis	Na_2SO_4–$Ni_3V_2O_8$	NiO–$Ni_3V_2O_8$ Na_2SO_4	NiO–$Ni_3V_2O_8$ Na_2SO_4

their action and the influence of sodium and SO_3 pressure on V_2O_5-induced hot corrosion.[22]

The search for other refractory materials able to trap vanadium in the flame or on the mechanical parts and having a higher melting temperature, leading to increased performance of combustion equipment burning contaminated fuels, is an ongoing challange.

This paper studies the effect of nickel additive on the chemistry of the sodium–vanadium-based ash materials. A comprehensive study of the formation of the nickel orthovanadate compound ($Ni_3V_2O_8$) in comparison with magnesium orthovanadate has been carried out in these melts as a function of sodium and SO_x content. Initially, analysis and thermochemical studies of the reactions in these corrosive ash materials were performed. Then, the inhibiting efficiency of nickel was evaluated by kinetic thermogravimetric studies of superalloys coated with synthetic ash materials.

Experimental

Thermochemical experiments. NiO, MgO, Na_2SO_4 and V_2O_5 were obtained from Aldrich. The thermochemical study of synthetic ash materials was conducted on mixtures of oxides that were ground and placed in tube furnaces at 850 °C for 3 days in air containing 150 ppmw of SO_2 with a flow rate of 3 L h^{-1}. Then, the reaction products were quenched in air, subjected to metallographic observations and analysed by X-ray diffraction at room temperature (θ–2θ Bruker diffractometer using Cu-Kα radiation and equipped with a DACO MP acquisition system). The XRD diffractograms were analysed using DIFFRAC AT software with the JCPDS databank.

Metallographic cross-sections were prepared by embedding the sample in epoxy resin under vacuum, followed by polishing in non-aqueous solvent, and were analysed by energy-dispersive spectroscopy (EDS) in a scanning electron microscope (SEM; Hitachi 250 equipped with a Kevex Sigma energy-dispersive X-ray spectrometer). The thermal behaviour of some ash materials was studied by differential thermal analysis (DTA; heating rate: 1 °C min^{-1}), to identify low melting point phases, coupled with *in situ* thermogravimetric analysis (Setaram TGA92). The synthesis of pure $Ni_3V_2O_8$ and $Mg_3V_2O_8$ compounds was carried out at 1000 °C in air with an NiO or MgO and V_2O_5 melt previously ground and pressed.

Corrosion tests. The superalloy selected for this study was GTD111 (composition: Ni base, Cr 14 wt%, Co 9.5 wt%).

The thermogravimetric tests were performed in a thermobalance (Setaram G85) at 850, 700 and 550 °C for 100 h using parallelepiped metallic samples (GTD111 alloy) covered by an oxide deposit of 5 mg cm^{-2} simulating the corrosive ash layer (10 × 10 × 2 mm). The samples were hung with a platinum wire in a flow of air containing 150 ppmw of SO_2 with a flow rate of 3 L h^{-1}. The metallographic cross-sections of the oxidised samples were observed by SEM and analysed by EDS. The synthetic ash deposits were applied by spraying an aqueous solution containing corrosive and inhibiting elements on the metallic samples previously heated at 400 °C. The sprayed aqueous solutions were prepared to generate a reproducible content of sodium, sulfur and vanadium (V_2O_5 : Na_2SO_4 = 70 : 30 by mass) and to reach the desired Ni/V or Mg/V ratios (by mass) in the deposit. The solutions contained V_2O_5 in suspension and $Ni(NO_3)_2{\cdot}6H_2O$, $Mg(NO_3)_2{\cdot}6H_2O$ and Na_2SO_4 dissolved in deionised water.

To express the effectiveness with which MgO or NiO inhibits vanadium-induced hot corrosion, inhibitor efficiency may be calculated as follows:

$$I = \frac{WG_1 - WG_2}{WG_1} \times 100$$

where I is the inhibitor efficiency (%), and WG_1 and WG_2 are the weight gain of the sample (mg cm^{-2} per 100 h) without and with inhibitor, respectively.

Results

According to the literature,[17–22] the inhibiting efficiency of an M^{2+} cation for vanadium-induced hot corrosion is directly linked to the thermodynamic and kinetic properties of the reaction that yields the $M_3V_2O_8$ refractory orthovanadate in molten sodium sulfate, which constitutes the main component of the ash materials. Hence, the reactivity between NiO or MgO and V_2O_5 has been studied in a variety of conditions to evaluate their inhibition efficiency.

Reactions of V_2O_5 with NiO or MgO in sodium sulfate

Table 1 summarises the results of XRD analysis of different oxide melts with a fixed Na/V ratio of 1.5. Results show that the reaction between MgO and V_2O_5 under stoichiometric conditions to form $Mg_3V_2O_8$ (Mg/V = 0.7) is greatly limited by the presence of sodium sulfate (Na/V = 1.5). Even in presence of a large excess of magnesium oxide (Mg/V = 10), the formation of the orthovanadate $Mg_3V_2O_8$ seems to be impossible under these conditions. Indeed, some of the MgO is transformed into a mixed sulfate, $Na_6Mg(SO_4)_4$, another fraction forms the mixed vanadate $NaMg_4(VO_4)_3$ and a small amount of the MgO remains free after 3 days at 850 °C. The compactness and the poorly crystallised aspect of the magnesium-based samples indicate that they are more or less completely molten at 850 °C. The differential thermal analysis trace in Fig. 1(b) shows that these two compounds have very low melting points: 510 °C for $NaMg_4(VO_4)_3$ and 660 °C $Na_6Mg(SO_4)_4$.

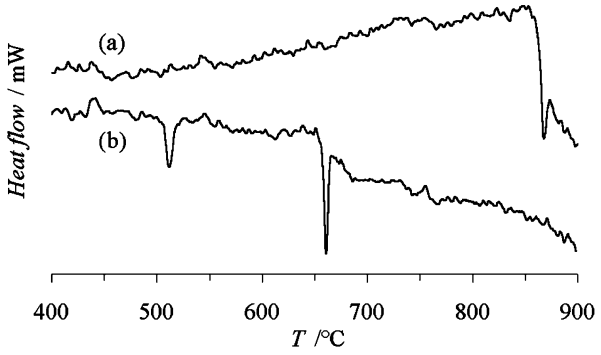

Fig. 1 DTA curves obtained when heating oxide melts with compositions (a) Na/V = 1.5, Ni/V = 2.25 and (b) Na/V = 1.5, Mg/V = 3, after 3 days at 850 °C in air containing 150 ppmw SO_3.

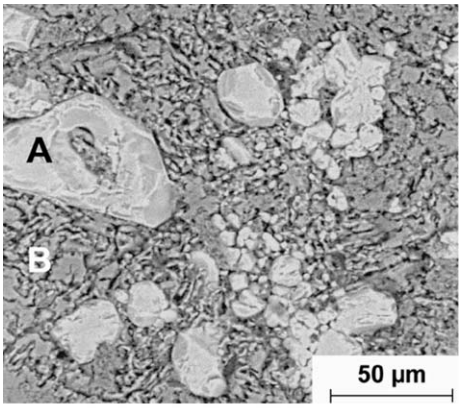

A : MgO - $NaMg_4(VO_4)_3$
B : $Na_6Mg(SO_4)_4$

a)

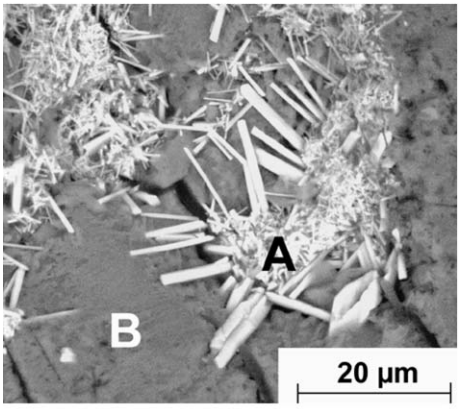

A : NiO - $Ni_3V_2O_8$
B : Na_2SO_4

b)

Fig. 2 SEM metallography of oxide melts with compositions (a) Mg/V = 3, Na/V = 1.5 and (b) Ni/V = 2.25, Na/V = 1.5, after 3 days at 850 °C in air containing 150 ppmw SO_3.

In contrast to magnesium orthovanadate, the formation of nickel orthovanadate ($Ni_3V_2O_8$) is complete at any Ni/V ratio which exceeds the stoichiometric ratio of $Ni_3V_2O_8$ (Ni/V = 1.74), and is unaffected by either the presence of sodium sulfate or by SO_3 gas (Table 1). Indeed, for these melts, the DTA analysis shows that the only molten compound that exists between 400 and 900 °C is sodium sulfate at 850 °C [Fig. 1(a)]. Moreover, the metallographic observations reveal well-crystallised platelet or needle-like crystals of $Ni_3V_2O_8$ in the sodium sulfate matrix [Fig. 2(b)].

Table 2 presents the effect of sodium for two particular compositions: Ni/V = 2.25 and Mg/V = 3, which correspond to the practical ratios in the case of corrosion inhibition in gas turbines. The XRD results and the metallographic observations indicate that the formation of $Ni_3V_2O_8$ with an Ni/V ratio of 2.25 is very effective, whatever the sodium content in the melt [Fig. 3(b)]. In contrast, the $Mg_3V_2O_8$ refractory material is only formed at a very low Na/V ratio (0.15), whereas the

Table 2 X-Ray diffraction analysis of different oxide melts after 3 days at 850 °C in air containing 150 ppmw of SO_3, as a function of Na/V ratio

Na/V ratio	Ni/V = 2.25	Mg/V = 3
0.15	$NiO–Ni_3V_2O_8$	$MgO–Mg_3V_2O_8$
1.5	$NiO–Ni_3V_2O_8$	$MgO–Na_6Mg(SO_4)_4$
	Na_2SO_4	$NaMg_4(VO_4)_3$
15	Na_2SO_4	$Na_2SO_4–MgO$
	NiO	$Mg_2V_2O_7–Na_6Mg(SO_4)_4$
	$Ni_3V_2O_8$	$NaMg_4(VO_4)_3$

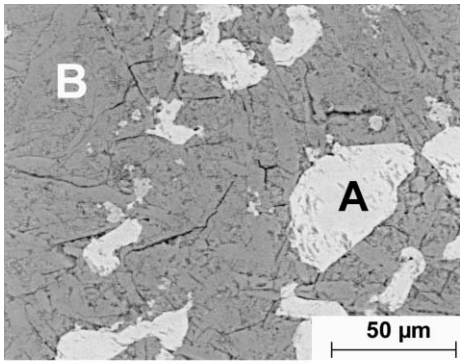

A : $Mg_2V_2O_7$ - $NaMg_4(VO_4)_3$
B : Na_2SO_4 – MgO - $Na_6Mg(SO_4)_4$

a)

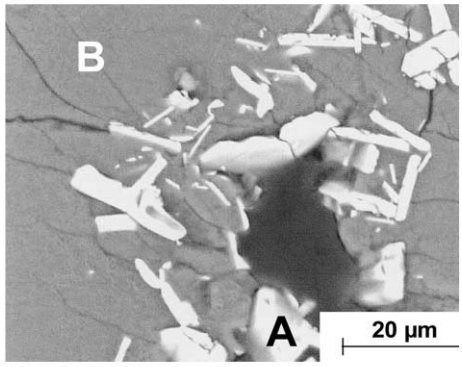

A : $Ni_3V_2O_8$
B : Na_2SO_4

b)

Fig. 3 SEM metallography of oxide melts with compositions (a) Mg/V = 3, Na/V = 15 and (b) Ni/V = 2.25, Na/V = 15, after 3 days at 850 °C in air containing 150 ppmw SO_3.

formation of low melting point compounds [$Na_6Mg(SO_4)_4$ and $NaMg_4(VO_4)_3$] is predominant at higher Na/V ratios. Such salts induce the fusion and compaction of the ash materials after 3 days at 850 °C [Fig. 3(a)]. So, for the Mg/V = 3 ratio commonly used in gas turbines, the quantitative formation of $Mg_3V_2O_8$ requires an Na/V ratio as low as 0.15 in the ash materials.

To study the stability of the metal vanadates, $Mg_3V_2O_8$ and $Ni_3V_2O_8$ were mixed with Na_2SO_4 in presence of air containing 150 ppmw of SO_3. After 3 days at 850 °C, XRD and metallographic observations reveal that $Ni_3V_2O_8$ remains stable, whereas $Mg_3V_2O_8$ is completely transformed into $Na_6Mg(SO_4)_4$ and $NaMg_4(VO_4)_3$, which confirms the instability of $Mg_3V_2O_8$ in presence of sodium sulfate.

Reactions of $NaVO_3$ with NiO or MgO

Without SO_3 pressure, the corrosive ash materials constituted by an $Na_2SO_4–V_2O_5$ melt leads to the formation of sodium metavanadate, $NaVO_3$, according to the literature.[2]

The reactivity of $NaVO_3$ with NiO and MgO for 3 days at 850 °C in the absence of SO_3 was studied and revealed the following: (i) there is no reaction between NiO and $NaVO_3$, whatever the Ni/V ratio (Ni/V = 1.74 and Ni/V = 2.25). (ii) In contrast, the XRD and metallographic analyses show that MgO reacts with $NaVO_3$ to form the mixed vanadate $NaMg_4(VO_4)_3$ and the sodium orthovanadate Na_3VO_4.

Corrosion study by thermogravimetric analysis

The corrosion study has been performed with synthetic ash materials with an Ni/V ratio of 2.25 deposited onto GTD111 alloys; the Ni/V ratio corresponds to an excess of nickel as

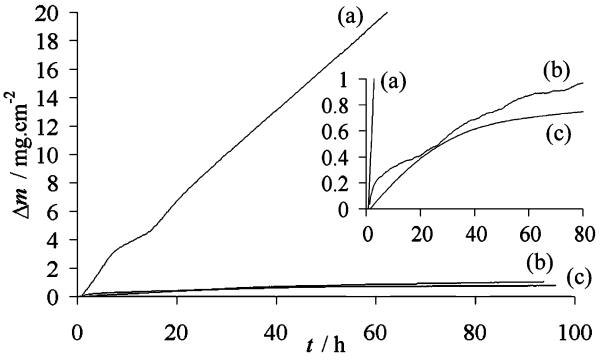

Fig. 4 Weight gain of GTD111 samples covered with synthetic ash deposits of compositions (a) Na/V = 1.5, (b) Na/V = 1.5, Mg/V = 3 and (c) Na/V = 1.5, Ni/V = 2.25, oxidised at 850 °C in a flow of air containing 150 ppmw SO_3.

compared to the $Ni_3V_2O_8$ stoichiometric ratio (Ni/V = 1.74). The inhibiting effect provided by this Ni/V ratio has been compared to that of the classical Mg/V ratio (Mg/V = 3) that is used in practice for power-generating gas turbines.

The weight gain of a GTD111 sample covered with synthetic ash deposit is plotted *versus* time at 850 °C in Fig. 4. In this environment, the weight increase is ten times larger for the uninhibited sample than for the inhibited ones, and approximately linear over a period of 100 h. This very high corrosion rate generates a thick layer containing a complex oxide–sulfate–vanadate melt and a large zone of internal sulfuration and oxidation, with some porosity appearing in the metal bulk [Fig. 5(a)]. For the Ni-inhibited sample, the weight gain is low and obeys an almost parabolic law. Metallographic cross-sections demonstrate that this low rate results from the build-up of a continuous and protective Cr_2O_3 layer upon the metal surface. At the same time, the vanadium species present in the ash deposit forms a porous and brittle layer consisting of the $Ni_3V_2O_8$ refractory compound and Na_2SO_4 [Fig. 5(b)]. For the Mg-inhibited sample, the weight gain curve is also approximately parabolic, but with some distortions as compared with the Ni-inhibited sample. Indeed, as can be seen in Fig. 5(c), the Cr_2O_3 layer is less continuous and seems locally dissolved by the external ash material composed of MgO, $Na_6Mg(SO_4)_4$ and $NaMg_4(VO_4)_3$. It is important to note that the ash deposit on the Mg-inhibited sample was found to be harder and more compact than that on the Ni-inhibited one. However, the two inhibitors dramatically decrease the corrosion level and the depth of internal sulfuration/oxidation, and their inhibition efficiencies are similar (96% for magnesium and 97% for nickel), despite the differences in the metallographical cross-section aspects between the two inhibitors.

The corrosion rate of GTD111 at 700 °C is lower than at 850 °C (Fig. 6). In presence of nickel, the weight gain is approximately halved and the aspect of the metallographic cross-section is similar to that at 850 °C [Fig. 5(b)]: a very thin layer of Cr_2O_3 and a porous ash deposit of $Ni_3V_2O_8$ and Na_2SO_4 [Fig. 7(a)]. For the Mg-inhibited sample, the high weight gain is partially due to the fast transformation of MgO into $MgSO_4$, which induces the formation of a more compact deposit, as can be seen in Fig. 7(b). Hence, the thermogravimetric data in these temperature conditions is representative of both the metallic corrosion and the sulfation of the ash material (Fig. 6).

At 550 °C, the corrosion rate of GTD111 samples is very low after 100 h exposure and the weight gain of the sample is mainly due to the sulfation of magnesium or nickel oxide (Fig. 8). Indeed, the cross-sections of the Ni-inhibited sample show that the partial transformation of nickel oxide into nickel sulfate leads to the formation of an Na_2SO_4–$NiSO_4$ melt [Fig. 9(a)]. Identically to the test at 700 °C, the sulfation of a large fraction

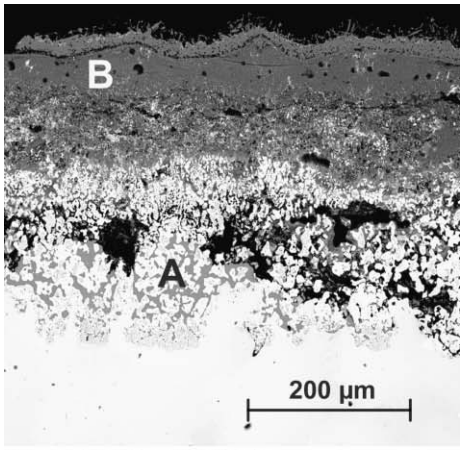

A : Porosity and internal oxidation
B : Oxide, sulfate vanadate melt.

a)

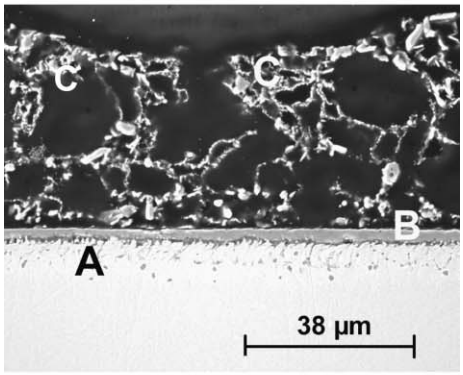

A : Internal oxidation
B : Cr_2O_3 layer
C : $Ni_3V_2O_8$ and Na_2SO_4

b)

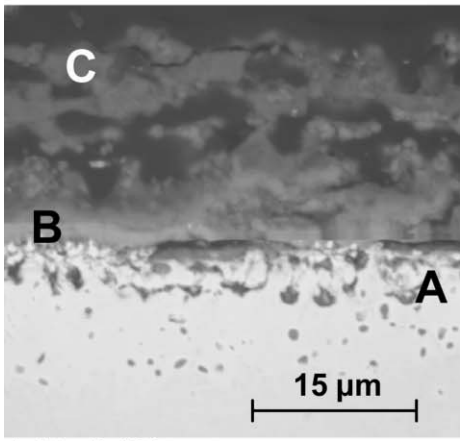

A : Internal oxidation
B : Cr_2O_3 layer
C : melt of MgO, $Na_6Mg(SO_4)_4$, $NaMg_4(VO_4)_3$

c)

Fig. 5 SEM micrographs of GTD111 samples covered with synthetic ash deposits of compositions (a) Na/V = 1.5, (b) Na/V = 1.5, Mg/V = 3 and (c) Na/V = 1.5, Ni/V = 2.25, oxidised at 850 °C in a flow of air containing 150 ppmw SO_3.

of magnesium oxide is responsible for the weight gain of this sample and for the compactness of the ash material on the metal, composed of a Na_2SO_4–$MgSO_4$ melt and a sodium–magnesium vanadate, as can be seen in Fig. 9(b).

It is noteworthy that, even at relatively low temperatures (550 or 700 °C), nickel oxide reacts with vanadium pentoxide to form $Ni_3V_2O_8$ and the extent of NiO sulfation remains low. For magnesium, above this temperature range, the high degree of MgO to $MgSO_4$ conversion is responsible for the compactness and the hardness of the magnesium-based ash material.

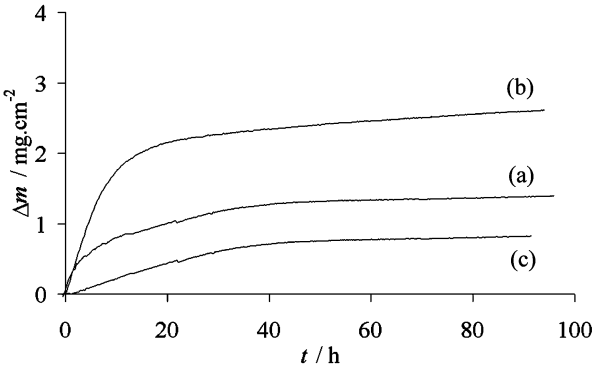

Fig. 6 Weight gain of GTD111 samples covered with synthetic ash deposits of compositions (a) Na/V = 1.5, (b) Na/V = 1.5, Mg/V = 3 and (c) Na/V = 1.5, Ni/V = 2.25, oxidised at 700 °C in a flow of air containing 150 ppmw SO_3.

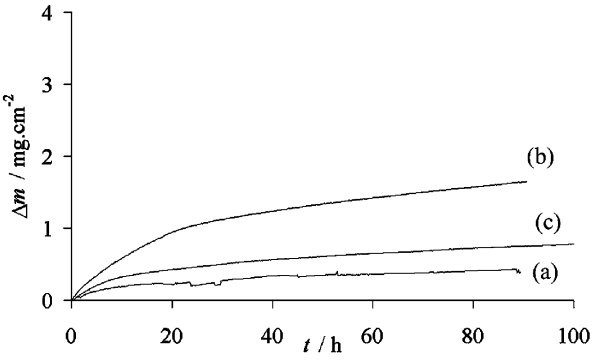

Fig. 8 Weight gain of GTD111 samples covered with synthetic ash deposits of compositions (a) Na/V = 1.5, (b) Na/V = 1.5, Mg/V = 3 and (c) Na/V = 1.5, Ni/V = 2.25, oxidised at 550 °C in a flow of air containing150 ppmw SO_3.

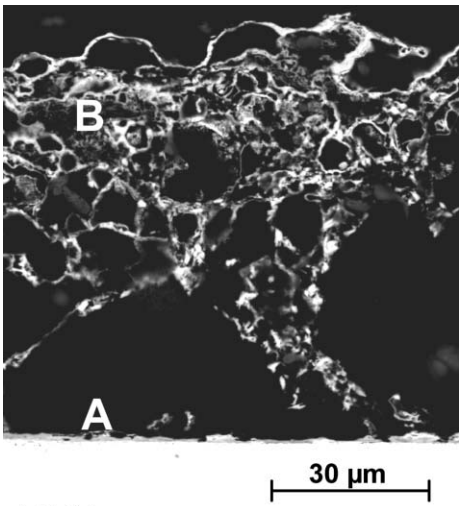

A: Cr_2O_3 layer
B : $Ni_3V_2O_8$ and Na_2SO_4

a)

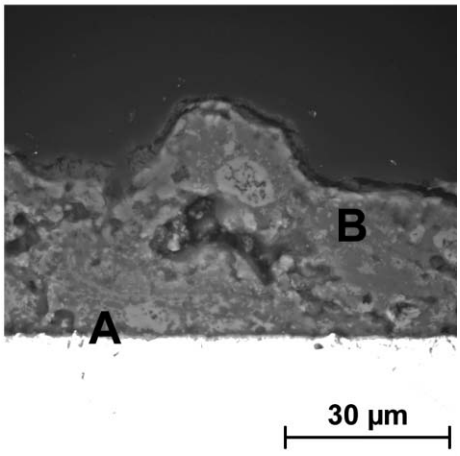

A: Cr_2O_3 layer
B : melt of MgO, $Na_6Mg(SO_4)_4$, $NaMg_4(VO_4)_3$

b)

Fig. 7 SEM micrographs of GTD111 samples covered with synthetic ash deposits of compositions (a) Na/V = 1.5, Ni/V = 2.25 and (b) Na/V = 1.5, Mg/V = 3, oxidised at 700 °C in a flow of air containing 150 ppmw SO_3.

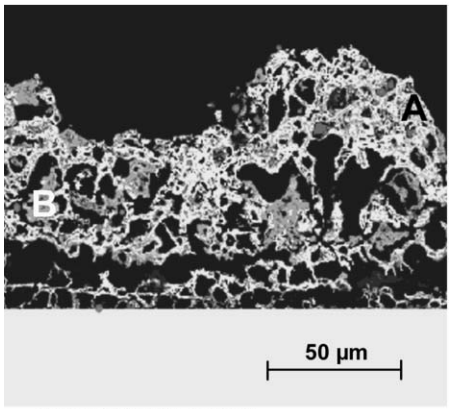

A : melt of $Ni_3V_2O_8$ and NiO
B : melt of Na_2SO_4 and $NiSO_4$

a)

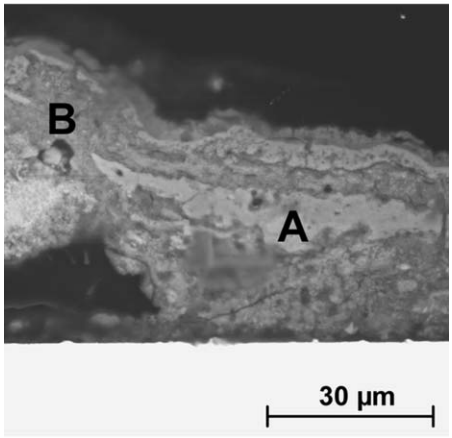

A : melt of sodium and magnesium vanadate
B : melt of Na_2SO_4 and $MgSO_4$

b)

Fig. 9 SEM micrographs of GTD111 samples covered with synthetic ash deposits of compositions (a) Na/V = 1.5, Ni/V = 2.25 and (b) Na/V = 1.5, Mg/V = 3, oxidised at 550 °C in a flow of air containing 150 ppmw SO_3.

In summary, the results clearly show that nickel oxide is as efficient as magnesium oxide in inhibiting the vanadium-induced hot corrosion of superalloys in thermal facilities over a large range of temperature. Nevertheless, the study of the oxide interactions and the metallographic analysis of corroded samples demonstrate that the mechanism of corrosion inhibition for magnesium seems to be more complex that involving nickel.

Discussion

The reactions in corrosive Na_2SO_4–V_2O_5 ash-materials can be explained in terms of acid–base reaction in presence or absence

of SO_3 gas.[23] Indeed the reactions in Na_2SO_4 matrix at high temperature can be understood at the light of the Lux–Flood acid-base theory.[24]

$$\text{base} = \text{acid} + O^{2-}$$

thus, in an SO_3-rich environment,

$$SO_4^{2-} = SO_3 + O^{2-}$$

As noted by Luthra and Spacil,[2] the composition of the Na_2SO_4–V_2O_5 ash is mainly determined by the acid (V_2O_5)–base (Na_2SO_4) reaction

$$Na_2SO_4 + V_2O_5 = 2NaVO_3 + SO_3$$

which is easily shifted towards the left side in the presence of SO_3. The very acidic properties of this V_2O_5-based ash material lead to fast attack of superalloys due to the rapid dissolution of the Cr_2O_3 protective layer into liquid $CrVO_4$ through an acid (V_2O_5)–base (Cr_2O_3) reaction and fast VO_3^-/VO_4^{3-} ionic exchange. This type of corrosion is characterised in kinetics terms by a linear weight gain for the sample. Simultaneously, the continuous dissolution of the protective layer induces an important internal oxidation and sulfidation process.

The addition of MgO or NiO to the ash deposit stabilises the Cr_2O_3 protective layer. Indeed, the acidity of the Na_2SO_4–V_2O_5 ash material appears to be modified by NiO or MgO, nevertheless, the mechanism seems to be different for the the two oxides, as revealed by XRD and metallographical analysis.

For nickel oxide, the inhibiting effect is clearly due to the fast reaction of NiO with V_2O_5 in a sodium sulfate matrix, which allows the vanadium species to be trapped into the refractory $Ni_3V_2O_8$ material (T_f = 1310 °C[16]). This reaction is not sensitive to the sodium content, and can be written as follows:

$$3NiO(s) + V_2O_5(l) + Na_2SO_4(l) \rightarrow Ni_3V_2O_8(s) + Na_2SO_4(l)$$

This mechanism is very simple and leads to the formation of a porous, friable deposit, which is easily removed, as noted during the corrosion tests.

Nevertheless, in presence of $NaVO_3$ in pure air, no reactions were observed with nickel oxide. This tends to demonstrate that the driving force to form $Ni_3V_2O_8$ in these corrosive media is the difference in the acidity of the two reactants, vanadium oxide and NiO. V_2O_5 is much more acidic than $NaVO_3$, according to Rapp and Zhang,[10] so, the difference in acidity between $NaVO_3$ and NiO is too low to allow rapid and quantitative formation of the refractory $Ni_3V_2O_8$ compound.

In contrast to nickel oxide, the effect of magnesium oxide in the presence of sodium appears to be more complex. Indeed, MgO can be considered as a strong base according to the Lux–Flood acid–base theory, and its reaction with acidic V_2O_5 to form $Mg_3V_2O_8$ should be very fast and quantitative. Nevertheless, under these conditions, the formation of two different salts, $Na_6Mg(SO_4)_4$ and $NaMg_4(VO_4)_3$, can be observed, which can be written as follows:

$$9MgO(s) + 3V_2O_5(l) + 4Na_2SO_4(l) \rightarrow 2\ NaMg_4(VO_4)_3(l) + Na_6Mg(SO_4)_4(l)$$

Despite the formation of two liquid phases, according to the DTA experiments, the corrosiveness of this MgO-based ash material is much lower than the non-inhibited ash and allows the formation of the protective Cr_2O_3 layer on the superalloy. Therefore, in presence of sodium, the action of the magnesium additive does not involve trapping vanadate anions into a refractory compound, in contrast to the actrion of the nickel additive. Indeed, $Mg_3V_2O_8$ seems to be basic enough to react with the acidic Na_2SO_4/SO_3 medium, according to our results. Hence, even if MgO does not form $Mg_3V_2O_8$ in this ash material, the O^{2-}-donor character of magnesium stabilises the orthovanadate VO_4^{3-} anions into an $NaMg_4(VO_4)_3$ liquid phase, according to the equilibrium

$$VO_3^- + O^{2-} \rightleftharpoons VO_4^{3-}$$

This reaction reduces the ionic exchange of O^{2-} through the VO_4^{3-}/VO_3^- acid–base couple and dramatically reduces the acidic character of the vanadium-based ash material. At the same time, the partial sulfation of MgO lowers the partial pressure of SO_3 and, thus, the acidity of the medium (decrease in pO^{2-}), which also favours the stabilisation of the VO_4^{3-} anions. Simultaneously, the oxidising power of the VO_3^-/VO_3^{2-} couple decreases as the oxidant species get complexed by O^{2-} anions.

Consequently, even if, in presence of sodium, the addition of MgO does not lead to the formation of a $Mg_3V_2O_8$ refractory compound, the stabilisation of vanadium into orthovanadate (VO_4^{3-}) anions in a mixed vanadate compound $NaMg_4(VO_4)_3$ inhibits the acidic dissolution of the Cr_2O_3 protective layer and, thus, decreases the corrosiveness of the (Na–V)-based ash materials.

Finally, the difference in behaviour between NiO- and MgO-inhibited ash is due to the different acid–base properties of $Mg_3V_2O_8$ and $Ni_3V_2O_8$. Indeed, $Mg_3V_2O_8$ is too basic to be stable in the Na_2SO_4–SO_3 medium, whereas $Ni_3V_2O_8$ is stable under these conditions. This property does not affect the efficiency of MgO as a corrosion inhibitor, but has some important consequences for its use in gas turbines. The formation of liquid $NaMg_4(VO_4)_3$ and liquid $Na_6Mg(SO_4)_4$, which act as binders between the ash particles, is responsible for the compactness of the deposit and the impervious coverage of the metallic parts. In addition, the large excess of magnesium required to counterbalance the sulfation reaction increases this phenomenon. Thus, the presence of this compacted ash material means that periodic washing of the hot gas path of gas turbines is required to remove it, so limiting the availability of the machine. In contrast, the NiO-inhibited ash material leads to the formation of friable and brittle deposits of $Ni_3V_2O_8$, which can be easily peeled off from the metallic surfaces.

Conclusion

The chemistry of oxides in (Na–V)-based ash materials are predominantly controlled by Lux–Flood-type reactions and are explainable in terms of the relative acid–base properties of the reactants.

In an Na_2SO_4–SO_3 environment, the addition of NiO leads to the formation of $Ni_3V_2O_8$, a refractory compound which dramatically reduces the corrosiveness of the ash materials by trapping vanadium. Although, with an extremely low pressure of SO_3, the presence of $NaVO_3$ in the ash material can prevent the formation of $Ni_3V_2O_8$ because of the smal difference in acidity between the reactants; in practice, the Na/S ratio in fuels is always sufficiently large to ensure the presence of Na_2SO_4, to the detriment of $NaVO_3$.

Even if MgO and NiO have similar efficiencies from the corrosion point of view, the effect of MgO on the chemistry of the (Na–V)-based ash materials is twofold: (i) the basic power of MgO allows the vanadium to be stabilsed into orthovanadate anions VO_4^{3-} [$NaMg_4(VO_4)_3$], which dramatically reduces the corrosive effect of the more acidic vanadium species, VO_3^- and V_2O_5. (ii) The formation of two liquid phases at 850 °C, $Na_6Mg(SO_4)_4$ and $NaMg_4(VO_4)_3$, which act as binders in the deposit, induce compaction of the ash material.

In conclusion, nickel oxide can successfully substitute for magnesium as an inhibitor of hot vanadium corrosion, even in

the presence of relatively large concentrations of sodium. The main advantages of nickel with respect to magnesium are the high melting point of $Ni_3V_2O_8$, the ease with which the ash material can be removed and the absence of NiO sulfation in the temperature range under consideration.

References

1 F. J. Kohl, G. J. Santoro, C. A. Stearns and G. C. Frybourg, *J. Electrochem. Soc.*, 1979, **126**, 1054–1061.
2 K. L. Luthra and H. S. Spacil, *J. Electrochem. Soc.*, 1982, **129**, 649–656.
3 P. Kofstad, *High Temperature Corrosion*, Elsevier Applied Science, London, 1988, p. 494.
4 N. S. Bornstein, M. A. DeCrescente and H. A. Roth, *Metall. Trans.*, 1973, **4**, 1799–1810.
5 C. O. Chang and R. A. Rapp, *J. Electrochem. Soc.*, 1986, **133**, 1636–1641.
6 M. Franke and J. Winnick, *J. Electroanal. Chem.*, 1987, **238**, 163–182.
7 M. Seirstein and P. Kofstad, *Mater. Sci. Technol.*, 1987, **3**, 576–583.
8 E. Otero, A. Pardo, J. Hernaes and F. J. Perez, *Corros. Sci.*, 1992, **33**, 1747–1757.
9 N. Otsuka and R. A. Rapp, *J. Electrochem. Soc.*, 1990, **137**, 54–60.
10 R. A. Rapp and Y. S. Zhang, *J. Met.*, 1994, Dec., 47–55.
11 D. Z. Shi, J. C. Nava and R. A. Rapp, *Proc. Symp. High Temp. Mater. Chem. IV*, 1987, **88**, 1–25.
12 I. B. Singh, *Indian J. Chem. Technol.*, 1998, **5**, 163–165.
13 Y-S Hwang and R. A. Rapp, *Corrosion*, 1989, **45**, 933–937.
14 S. Y. Lee, W. E. Young and G. Vermes, ASME paper no. 73-GT-1, American Society of Mechanical Engineers, New York, 1973.
15 M. Moliere, ASME paper no. 98-GT-231, American Society of Mechanical Engineers, New York, 1998.
16 *Phase Diagrams for Ceramicists*, National Bureau of Standards, The American Ceramic Society, New York, 1964, p. 114.
17 W. R. May, M. J. Zetlmeisl and L. Bsharah, *Ind. Eng. Chem. Prod. Res. Dev.*, 1973, **12**, 140–144.
18 W. R. May, M. J. Zetlmeisl, L. Bsharah and R. R. Annand, *Ind. Eng. Chem. Prod. Res. Dev.*, 1973, **12**, 145–149.
19 W. R. May, M. J. Zetlmeisl and R. R. Annand, *J. Eng. Power*, 1976, **98**, 506–510.
20 T. N. Rhys-Jones, J. R. Nicholls and P. Hancock, *Corros. Sci.*, 1983, **23**, 139–149.
21 R. C. Kerby and J. R. Wilson, *Can. J. Chem.*, 1973, **51**, 1032–1040.
22 S. N. Tiwari and S. Prakash, *Mater. Sci. Technol.*, 1998, **14**, 467–472.
23 R. L. Jones, C. E. Williams and S. R. Jones, *J. Electrochem. Soc.*, 1986, **133**, 227–230.
24 H. Flood and T. Forland, *Acta Chem. Scand.*, 1947, **1**, 592–604.